

# The effect of ER4043 and ER5356 filler metal on welded Al 7075 by metal inert gas welding

M. N. M. Salleh, M. Ishak, L. H. Shah & S. R. A. Idris  
*Faculty of Mechanical Engineering,  
Universiti Malaysia Pahang, Malaysia*

## Abstract

Al 7075 is widely used in the automobile and aviation industry due to its light weight, strength, and good durability. Fusion welding such as metal inert gas (MIG) is commonly used in joining aluminium alloys. It was used because of its low cost and is generally used by welders. However, defects usually occurred using fusion welding because of improper welding parameters and the types of filler metal used. The purpose of the study is to investigate the effect of filler metal and welding parameters on the mechanical properties of welded Al 7075. The welding parameters used are current, voltage, welding speed, and Argon (Ar) as shielding gas. Two different types of filler metal, namely, Electrode Rod (ER) 4043 and ER5356 have been used. From microstructure analysis, the fusion zone (FZ) of a sample welded with ER4043 has a smaller grain size than that of one welded with ER5356. Both fillers produce equiaxed dendritic grain at FZ. Both samples welded with ER4043 and ER5356 have a lower hardness value than the heat affected zone (HAZ) and base metal (BM) due to the differences in their main elements where ER4043 is Al-Si and ER5356 is Al-Mg. The weld efficiency of a sample welded using ER5356 was 61% which was higher compared with a sample welded using ER4043, which is 43% and both samples were brittle fractured. The sample welded with ER5356 was fractured at HAZ due to porosity while the sample welded with ER4043 fractured at FZ due to the oxide inclusion at FZ.

*Keywords: Al 7075, ER4043, ER5356, MIG, mechanical properties, microstructure analysis.*

## 1 Introduction

Aluminium alloys 7075 (Al-Zn-Mg) have been utilized throughout aircraft and aerospace structure. This metal is heat treatable and the strongest and the most durable of aluminium alloys [1]. Al 7075 was largely used in the automobile and aerospace industry [2, 3]. In addition, connecting rods, axle shafts, rims, as metals in bumpers and door beams in car bodies are made from Al 7075 [4]. It has been used largely for the body of aircraft and for the fuel tank in spacecraft. This is due to its characteristics of being lightweight, strong and very durable and it also has good machinability [5]. TIG and MIG were mostly used in the joining process of aluminium alloys [6–10], but MIG welding was preferable since it is widely used for welding aluminium and produces a good weld quality [7]. Filler metal plays an important role in fusion welding since the selection of filler metal type can affect the welded joint. 7N01 alloys of 7000 series aluminium alloys with other aluminium alloys such as the 5000 and 6000 series where they are applicable as structural material in the automobile sector had been welded with filler wire ER5356 using the DCEP-MIG welding method [4, 7, 11]. This means that the common filler wire used for welding aluminium alloys is ER5356 (Al-Mg). The joining method used for this study is Direct Current Electrode Positive (DCEP) Pulse Metal Inert Gas (MIG). This research is to study the mechanical and microstructure of welded Al 7075 when welded with another type of filler metal which is ER4043 from the 4000 series of aluminium alloys (Al-Si). Thus, the mechanical properties and microstructure of a welded sample with ER4043 will be compared with ER5356. The welded Al 7075 aluminium alloys joint will undergo mechanical testing, such as the Vickers hardness test and tensile test as well as microstructure and EDX analysis in order to observe the microstructure after welding by ER4043 and ER5356. This investigation is also to distinguish the fracture behavior when welded with both fillers.

## 2 Experimental procedures

In this study, Al 7075 with 2 mm thickness was used and the chemical composition of Al 7075 as well as the filler wires is shown in Table 1. Al 7075 presents Zn and Mg as the major alloying element with 5.58% and 2.28%, respectively. ER4043 shows Si is the alloying element with 6.0% and ER5356 shows Mg is the alloying element for 5.5%. Al 7075 were cut in dimensions of  $150 \times 150 \times 2$  mm. An ASTM E8 tensile sample was produced from welded specimens using a CNC milling machine. The illustration for the tensile sample from the welded specimen is shown in Figure 1. The results of the tensile test were recorded in order to compare the strength between the parent metal Al 7075 with that welded by both fillers. Then, the welded sample was hot mounted for microstructure observation and Vickers' hardness testing. An optical microscope was used to observe the microstructure of a welded sample cross section. Based on Box-Behnken, 14 samples are needed for each experiment and due to the differences in chemical composition of fillers, the range of parameters for

current, voltage and welding speed are different. The listing of experimental parameters is shown in Table 2.

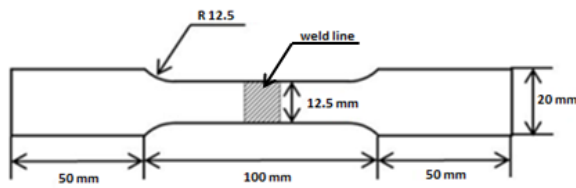


Figure 1: ASTM E8 tensile sample.

Table 1: Chemical composition of Al 7075 aluminium alloys and filler wire.

Element	Composition (wt%)		
	Al 7075	ER4043	ER5356
Mg	2.28	0.05	5.50
Zn	5.58	0.10	1.00
Si	0.07	6.00	0.25
Fe	0.27	0.80	0.40
Cu	1.60	–	–
Mn	0.02	–	–
Al	Bal.	Bal.	Bal.

Table 2: Welding conditions.

Working parameter	Description
Process	DCEP-Pulse MIG welding
Shielding gas	25 L/min-Ar
Workpiece dimension	Al 7075-150 × 150 × 2mm
Filler metal	ER4043, ER5356(1.0mm-diam)
Current	105–115 A (4043) 100–110 A (5356)
Voltage	17.5–18 V (4043) 16.0–20 V (5356)
Welding speed	3–5 mm/s (4043) 2–4 mm/s (5356)

### 3 Result and discussion

#### 3.1 Microstructure analysis

Figure 2 shows the microstructure of a welded Al 7075 cross section at three different locations using filler rod ER5356 and ER4043. For the base metal (BM) microstructure, it was found that the spheroidal particles which were the dark precipitates represented the MgZn elements and the light grey particles represented the FeAl<sub>3</sub> [12]. The grains elongated horizontally along one direction only. It was found that the equiaxed dendritic network grain presented at FZ of both samples welded by ER4043 and ER5356. The grain size at FZ was different for both samples. The average grain size of FZ, HAZ, and BM is presented in Table 3. The grain size in FZ for ER5356 was larger than the grain size for ER4043 with 99.50 $\mu$ m and 32.58 $\mu$ m, respectively. The microstructure at the partially melted zone (PMZ) which was the transition region between the FZ and HAZ was a typical coarse columnar grain [13]. This was due to the zone having deteriorated with the heat of welding during the melting and solidification process [7]. There was approximately similar average grain size in HAZ and BM for both samples.

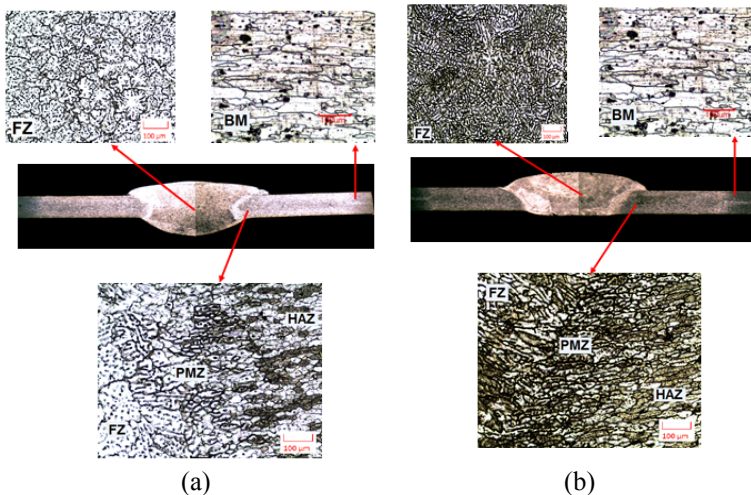


Figure 2: Microstructure image of welded cross section (a) Al 7075 with ER5356 and (b) Al 7075 with ER4043.

Table 3: Average grain size of microstructure.

Region	Average grain size ( $\mu$ m)	
	ER5356	ER4043
Fusion zone (FZ)	99.50	32.58
Heat affected zone (HAZ)	95.28	95.34
Base metal (BM)	131.24	131.20

### 3.2 EDX analysis

The energy dispersive X-ray (EDX) with spot analysis on FZ, HAZ and BM of the welded Al 7075 using fillers ER4043 and ER5356 has been conducted. The results for the base metal are tabulated in Table 4. Figure 3 shows the spot EDX analysis of the Al 7075 base metal. It was found that the atomic percentage of Al and Cu presents much higher than other elements (as shown in Table 4). It shows that the silverish spot was due to the Al-Cu compound which presented in Al 7075.

Table 4: Element concentration for Al 7075 base metal.

Point	Elements concentration (%)					
	Al	Zn	Mg	Cu	Fe	Si
1	41.1	1.3	1.3	33.0	8.0	2.0
2	90.9	4.2	3.5	–	–	1.4
3	90.3	4.0	3.4	–	–	1.6

At points 2 and 3, which are the grey parts showing a higher percentage of Zn element of 4.0%–4.2% and Mg element with 3.4%–3.5% (as shown in Table 4). It was found that points 2 and 3 were from the Al-Zn-Mg compound. From this result, it was proven that the sample used in this experiment was Al 7075, which is the Al-Zn-Mg-Cu aluminium alloy. The results from EDX were approximately the same as the results from the spectrometer for the BM (as shown in Table 1). There was no IMC interaction in BM of Al 7075 as the percentage of element found was normally present in this metal.

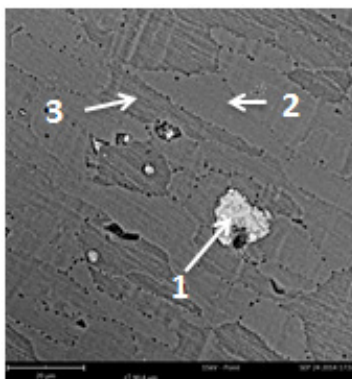


Figure 3: EDX spot analysis of Al 7075 base metal.

Table 5 shows the result of element concentration percentage and Figure 4 shows the EDX image at FZ and HAZ for a sample welded with filler ER5356.

In Figure 4(a), point 1 shows the silverish part in FZ where the atomic percentage of element Cu is 47.1% (highest), Al is 45.9 (2nd highest), and Mg is

2.8% (3rd highest) (as shown in Table 5). It was found that  $Cu_mAl_n$  compound presented relatively high at point 1. Point 2 shows the black spot which only has an atomic percentage of elements of Al with 95.1% (highest) and Mg with 4.9%. The black spot was proven to be the Al-Mg element. Point 3 shows the light grey spot which also only has Al and Mg elements. It was found that the particles of Al-Mg elements has the majority area from Figure 5(a) and a little amount of  $Cu_mAl_n$  compound present in the FZ. It was proven that some compound of  $Cu_mAl_n$  presented in FZ due to the IMC interaction because Cu element was originally from the BM element since it is not present as the alloying element in ER5356. In Figure 4(b), point 4 shows a silverish spot which has an atomic percentage of Al at 43.3% (highest); Cu is 19.3% (2nd highest), Fe is 9.9% (3rd highest), and Zn is 4.4% (4th highest). It was found that point 4 consists of  $Fe_mAl_n$  compound and the Cu element was normally found as the alloying element for Al 7075. Point 5 shows a dark grey part in HAZ which has Al with 95.0% (highest), Zn with 3.5% (2nd highest), and Mg with 1.5% (3rd highest). It was evident that the element presented in point 5 was Al-Zn-Mg which is the same element as the parent metal. Point 6 shows the black spot which has higher Mg concentration at 2.8% after 97.2% of Al (highest). From the EDX analysis

Table 5: Element concentration for welded Al 7075 using filler ER5356.

Point	Elements concentration (%)					
	Al	Zn	Mg	Cu	Fe	Si
1	45.9	–	2.8	47.1	–	–
2	95.1	–	4.9	–	–	–
3	95.6	–	4.4	–	–	–
4	43.3	4.4	1.8	19.3	9.9	2.4
5	95.0	3.5	1.5	–	–	–
6	97.2	–	2.8	–	–	–

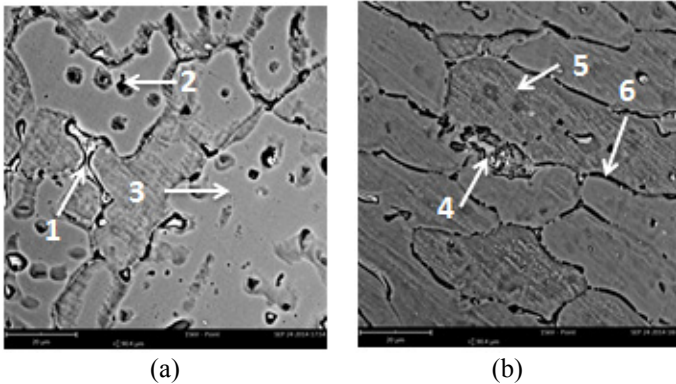


Figure 4: EDX spot analysis sample with ER5356: (a) fusion zone and (b) heat affected zone.

for the sample welded with filler ER5356, the element found in FZ was Al-Mg which came from the ER5356 element. At HAZ, the grey part was the majority area and it is from Al-Zn-Mg which is the base metal element with a small presence of  $Fe_mAl_n$  compound due to the presence of the Fe element in both the filler rod and parent metal which was 0.4% and 0.27%, respectively (as shown in Table 1).

Table 6 shows the result of element concentration percentage and Figure 5 presents the EDX image at FZ and HAZ for a sample welded with filler ER4043. In Figure 5(a), point 1 shows the silverish spot in the FZ with the atomic percentage of element Al being 56.6% (highest); Si is 23.1% (2nd highest), and Mg is 10.9% (3rd highest). It was shown that at point 1, the Al-Si element was from ER4043 which is from Al-Si alloy group. It was relatively high for the atomic percentage of Mg element in FZ due to the IMC interaction that occurs during the solidifying process and it produced an  $Al_mMg_n$  compound. Point 2 shows the dark elongated grain spot which contains an atomic percentage of Al with 39.6% (highest), Si with 20.4% (2nd highest), and Cu with 6.5% (3rd highest). It was proven that point 2 also consists of an Al-Si element as the major elements and Cu presents as the IMCs occur after the welding process with  $Al_mCu_n$  compound. Point 3 represents the light grey area which was the majority area in FZ where it has the element concentration of Al with 94.5% (highest), Si with 2.4% (2nd highest), and Mg and Zn represents approximately the same concentration percentages with 1.7% and 1.5%, respectively. It was found that in this region, the elements from a parent metal such as Mg and Zn were solidified together with the elements presented in the weld metal produced IMCs. It was proven that in FZ for a specimen welded with ER4043, the majority element was Al-Si which is the same alloying element of this filler where a small amount of  $Al_mCu_n$  and  $Al_mMg_n$  IMCs presented.

Table 6: Element concentration for welded Al 7075 using filler ER4043.

Point	Elements concentration (%)					
	Al	Zn	Mg	Cu	Fe	Si
1	56.6	1.2	10.9	5.0	3.2	23.1
2	39.6	1.6	2.1	6.5	–	20.4
3	94.5	1.5	1.7	–	–	2.4
4	25.4	6.7	2.1	40.7	2.7	3.9
5	96.2	–	3.8	–	–	–
6	81.0	9.5	3.5	6.0	–	–

From Figure 5(b), point 4 shows the silverish spot which consists of a percentage of the element Cu of 40.7% (highest); Al with 25.4% (2nd highest), and Zn with 6.7% (3rd highest). Therefore, point 4 has the element Cu as the majority element for the silverish spot where it was possibly from the Al 7075 parent metal. Point 5 shows the light grey parts from the HAZ where it has the atomic percentage of Al with 96.2% (highest) followed by Mg with 3.8%. It was proven that the light grey parts were from Al-Mg alloying elements from the

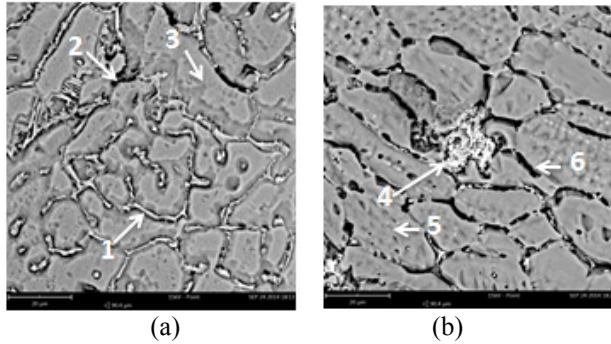


Figure 5: EDX spot analysis sample with ER4043: (a) fusion zone and (b) heat affected zone.

parent metal. Point 6 shows the black elongated spot in the HAZ microstructure. It was found that the atomic percentage of Al was the highest with 81.0% along with a small percentage of its alloying element such as Zn, Mg, and Cu (as shown in Table 6). It was proven that the HAZ of the sample welded using filler ER4043 has a very small amount of Si percentage. Therefore, the IMCs' interaction with the Al-Si compound does not occur for this sample due to the small amount of Si presented in HAZ. From the EDX results, the FZ region for the sample welded with filler ER5356 has the element of Al-Mg due to the larger area of greyish part. For its HAZ, it was found that it has an Al-Zn-Mg element the same as the Al 7075 base metal element. For the sample welded with filler ER4043, Si presents higher than other elements in FZ due to the major alloying element for ER4043 being Si. The HAZ region from this sample shows the element of Al-Zn-Mg being same as the Al 7075 base metal with some percentage of Si elements (as observed from the grey area in Figure 6).

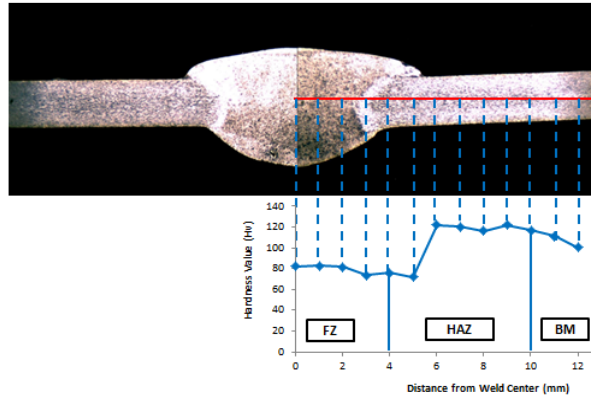
### 3.3 Vicker's hardness

Figure 6 shows the macrostructure images of samples with the UTS for both fillers. The average value of hardness test was presented in Table 7.

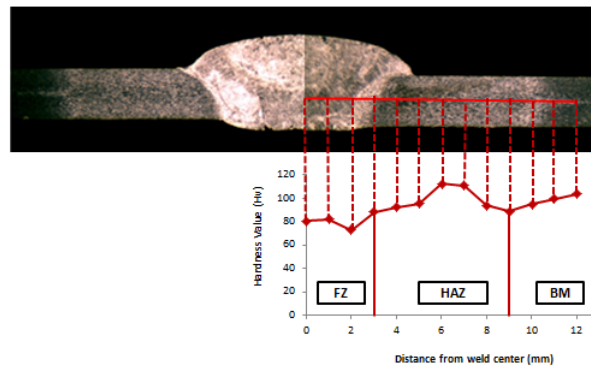
In Figure 6, it was found that the hardness value for the FZ region was lower than for the HAZ and BM. The average hardness values of the FZ region for both experiments were approximately similar, namely, 82.3 HV and 80.9 HV for the experiment with fillers ER5356 and ER4043, respectively. The average

Table 7: Average Vicker's hardness value.

Position	Average hardness value (HV)	
Filler	ER5356	ER4043
Fusion zone (FZ)	82.30	80.90
Heat affected zone (HAZ)	120.5	112.7
Base metal (BM)	109.7	103.6



(a)



(b)

Figure 6: Macrostructure image for Vickers' hardness test: (a) welded with ER5356 and (b) welded with ER4043.

hardness value at position HAZ was the highest for both welded samples with 120.5 HV and 112.7 HV for ER5356 and ER4043, respectively. The hardness value at HAZ was higher than the other region because the microstructure at HAZ was different due to the heat from the welding process that changes the microstructure of BM.

### 3.4 Tensile strength

The tensile test result was recorded and a graph of UTS is presented in Figure 7 for welded Al 7075. Welded specimen 7 from both experiments using fillers ER4043 and ER5356 recorded the highest UTS of 359.35 Mpa and 255.03 Mpa, respectively were compared with the UTS of the parent metal, which is 590.41 Mpa (as shown in Figure 7(a)). It was clearly observed from Figure 2 that at HAZ, the coarser columnar grain microstructure was produced starting from

the PMZ and the grain size at HAZ was also smaller than the grain size at BM for both samples. Although the grain size of FZ from the ER4043 experiment was smaller than that of ER5356, the hardness value was higher for FZ from the ER5356 experiment. It was due to the different groups of element of filler rod where for the 4xxx series from the Al-Si group, it has a Si element as its major alloying element which has a lower hardness than the 5xxx series from the Al-Mg group, which has the Mg element as its major alloying element. The 7xxx series from the Al-Mg-Zn group has the higher hardness value based on the results obtained from this testing. It was proven that the hardness value at HAZ and BM was higher than the FZ zone for both samples.

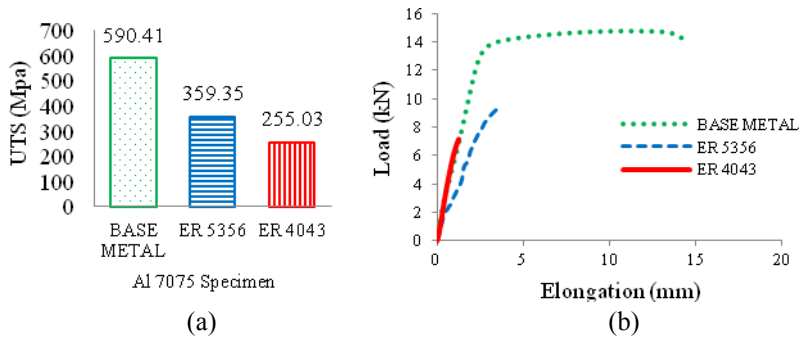


Figure 7: Ultimate tensile strength of Al 7075: (a) bar graph of UTS and (b) graph of load vs. elongation.

The weld efficiency of ER4043 and ER5356 was 43% and 61%, respectively showing that a sample welded with filler ER5356 has higher efficiency compared with a sample welded with filler ER4043. This is because filler ER5356 has Mg as its major alloying element which is stronger than Si, which is the major alloying element for filler ER4043. It was found that the UTS of a welded sample using ER4043 dropped by 56% from the UTS of the base metal while the welded sample using ER5356 dropped by 39%. The sample welded using filler ER5356 proved to be a better filler metal to weld Al 7075 compared with filler ER4043. The tensile test parameter was fixed – the speed at 0.083 mm/s and load at 50 kN – and it did not affect the UTS.

Figure 7(b) shows the load versus elongation plot for the tested sample. This graph shows the fracture behavior of the tested sample. Al 7075 base metal shows the different plot since it had plastic deformation before it fractured. This explained that Al 7075 has a ductile behavior due to the plastic deformation occurring before the fracture occurs. For a specimen welded with filler rod ER5356 and ER4043, there is no plastic deformation because of sudden fracturing occurring when certain loads were applied. It was found that after welding with ER4043 and ER5356, brittle behavior occurred.

### 3.5 Fracture analysis

The welded sample with ER5356 was fractured at the HAZ region. For ER4043, it was fractured at the FZ region. Figure 8 shows the SEM image of the fracture surfaces for both samples. It was found that both samples welded with ER4043 and ER5356 fractured at these regions due to the imperfection after the welding processes and it shows brittle fracture behavior.

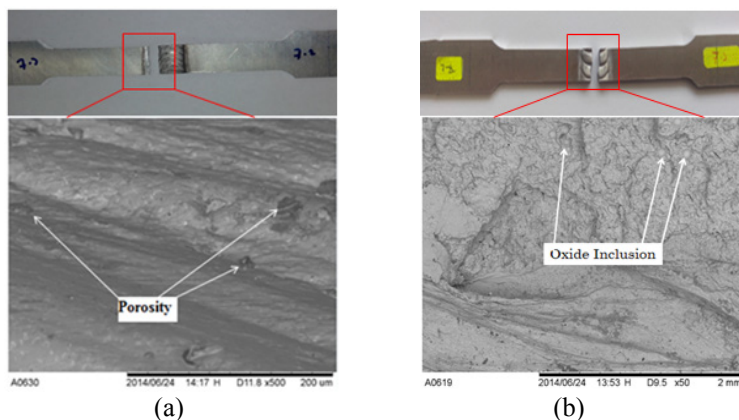


Figure 8: SEM image of fracture surface: (a) fracture surface of sample welded by ER5356 and (b) fracture surface of sample welded by ER4043.

Figure 8(a) shows that porosity presented in the HAZ and contributes to the fracture occurring at the HAZ region for a sample welded with filler ER5356. Meanwhile, the presence of oxide inclusion at the FZ due to the presence of oxide contributes to the welded samples of ER4043 being fractured at the FZ region (as shown in Figure 8(b)). It was found that a sample welded with ER4043 has a lower strength as it fractured at the FZ region due to the presence of oxide inclusion compared with a sample welded with ER5356 which fractured at the HAZ due to porosity defects.

## 4 Conclusion

The following points are concluded from this experiment for the effect of fillers ER4043 and ER5356 on the welded Al 7075:

1. It was observed that the microstructure sample in FZ was different for both fillers in terms of their grain size.
2. Smaller amounts of IMC compound such as  $Al_mCu_n$  were produced at the FZ for both fillers.
3. The hardness at the FZ region is lower compared with HAZ and BM for both fillers, while the weld efficiency when welded by ER5356 was higher than when welded by ER4043 when mechanical testing was investigated.

4. Fracture at HAZ and FZ occurs for a welded sample by ER5356 and ER4043, respectively. This is due to oxide inclusion for ER5356 and porosity for ER4043.

## References

- [1] T. Fakuda, "Weldability of 7000 series aluminium alloy materials," *Welding International*, vol. 26, pp. 256–269, 2012.
- [2] J. F. Tu and A. G. Paleocrassas, "Fatigue crack fusion in thin-sheet aluminum alloys AA7075-T6 using low-speed fiber laser welding," *Journal of Materials Processing Technology*, vol. 211, pp. 95–102, 2011.
- [3] S. Stano, T. Pfeifer, and M. Róžański, "Modern technologies of welding aluminium and its alloys", *Welding International*, vol. 28, pp. 91–99, 2014.
- [4] M. Ema, "Tensile strength of MIG-welded 7000 series aluminium alloy extrusions," *Welding International*, vol. 22, pp. 661–668, 2008.
- [5] K. G. Budinski and M. K. Budinski, *Engineering Materials, Properties and Selection*, 8th ed.: Prentice-Hall, 2005.
- [6] J. M. Fortain and S. Gadrey, "How to select a suitable shielding gas to improve the performance of MIG and TIG welding of aluminium alloys," *Welding International*, vol. 27, pp. 936–947, 2013.
- [7] S. M., M. N., A. D., and R. K. S., "Investigation of microstructure and mechanical properties of gtaw and gmaw joints of aa7075 aluminum alloy" *International Journal on Design and Manufacturing Technologies*, vol. 3, pp. 56–62, 2009.
- [8] F. Miyasaka, T. Okuda, and T. Ohji, "Effect of current wave-form on AC TIG welding of aluminium alloys," *Welding International*, vol. 19, pp. 370–374, 2005.
- [9] M. H. M. Temmar, T. Sahraoui, "Effect of post-weld aging treatment on mechanical properties of Tungsten Inert Gas welded low thickness 7075 aluminium alloy joints.," *Material and Design*, vol. 32, pp. 3532–3536, 2011.
- [10] V. R. V. Balasubramanian, G. Madhusudhan Reddy "Influences of pulsed current welding and post weld aging treatment on fatigue crack growth behaviour of AA7075 aluminium alloy joints.," *International Journal of Fatigue*, vol. 30, pp. 405–416, 2008.
- [11] M. Ema, "Tensile strength of MIG-welded aluminium alloys for structures," *Welding International*, vol. 22, pp. 199–205, 2008.
- [12] P. Z. Zhao and T. Tsuchida, "Effect of fabrication conditions and Cr, Zr contents on the grain structure of 7075 and 6061 aluminum alloys," *Materials Science and Engineering*, vol. A 499, pp. 78–82, 2009.
- [13] X. Cao, W. Wallace, J. P. Immarigeon, and C. Poon, "Research and Progress in Laser Welding of Wrought Aluminum Alloys. II. Metallurgical Microstructures, Defects, and Mechanical Properties," *Materials and Manufacturing Processes*, vol. 18, pp. 23–49, 2003.

